Acta Cryst C
STRUCTURAL
CHEMISTRY

ISSN 2053-2296

The study of interactions with a halogen atom: influence of NH_2 group insertion on the crystal structures of *meta*-bromonitrobenzene derivatives

Paulina H. Marek,[a,b] Mateusz Urban[a] and Izabela D. Madura[a]*

[a]Warsaw University of Technology, Faculty of Chemistry, Noakowskiego 3, 00-664 Warsaw, Poland, and [b]University of Warsaw, Faculty of Chemistry, Pasteura 1, 02-093 Warsaw, Poland. *Correspondence e-mail: izabela@ch.pw.edu.pl

Received 23 July 2018
Accepted 24 September 2018

Edited by G. P. A. Yap, University of Delaware, USA

Keywords: halogen bonds; hydrogen bonds; bromonitroanilines; Hirshfeld surface analysis; crystal structure; noncovalent interactions.

CCDC references: 1869457; 1869456

Supporting information: this article has supporting information at journals.iucr.org/c

Halogen atoms in molecular crystals may be involved in various interactions, often playing a very important role in structure stabilization. By introducing electron-donating groups, such as NH_2, the electron density of the molecule is changed and thus interactions with the bromine substituent may alter. Herein, the crystal structures of *meta*-bromonitrobenzene and its NH_2-substituted derivatives are analyzed. In all four described structures, namely *m*-bromonitrobenzene [Charlton & Trotter (1963). *Acta Cryst.* **16**, 313], 4-bromo-2-nitroaniline ($C_6H_5BrN_2O_2$, **1**), 2-bromo-6-nitroaniline (**2**) and 2-bromo-4-nitroaniline [Arshad *et al.* (2009). *Acta Cryst.* E**65**, o480], the Br atom is engaged in different interactions ($Br\cdots\pi$, $Br\cdots O$, $Br\cdots Br$ and $C-H\cdots Br$, respectively). The Hirshfeld surface analysis (HS) and Reduced Density Gradient NonCovalent Interaction (RDG NCI) plots are used to prove the relevance, directionality and stabilizing nature of these interactions. Their modifications have been associated with the position of the amino group in the molecular structure and its influence on charge distribution analyzed with electrostatic potential surfaces (EPS). The diversification of the interactions has been correlated with a σ-hole potential value that enables a switching of the Br-atom character from electrophilic to nucleophilic.

1. Introduction

Bromonitrobenzenes are a widely known group of compounds most often utilized in transition-metal-catalyzed C—C coupling reactions (*e.g.* Suzuki–Miaura) as building blocks for a large variety of target compounds (Hussain *et al.*, 2016). They are also precursors for brominated anilines (Tian *et al.*, 2017), which in turn are crucial intermediates and raw materials for the synthesis of fine chemicals, including medicines. Generally, a bromine substituent is often used to increase the lipophilicity of drugs, which directly translates into the nature of binding to biomolecular systems. Interactions, where a halogen atom interacts with electron-rich molecular fragments, *e.g.* a lone electron pair or π electrons, are nowadays recognized as halogen bonds (Desiraju *et al.*, 2013; Cavallo *et al.*, 2016). Usually, the halogen-bond donor is a small halogenated molecule, while one or more specific sites of a biomacromolecule (typically a protein) can act as acceptors (Cavallo *et al.*, 2016). It is worth underlining that Cl/Br$\cdots$aryl-π interactions were found to contribute significantly to binding affinity in the protein–ligand recognition process (Matter *et al.*, 2008). The formation of those interactions in solution was also proved (Sun *et al.*, 2017).

The anisotropic electron-density distribution around halogen atoms and the formation of the so-called σ-hole (Brinck *et al.*, 1992; Clark *et al.*, 2007) rises with the polariz-

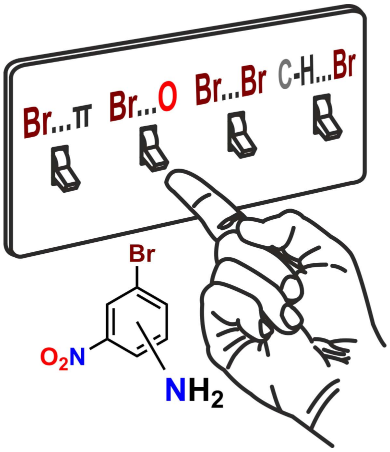

https://doi.org/10.1107/S2053229618013608

Table 1
Experimental details.

	1	**2**
Crystal data		
Chemical formula	$C_6H_5BrN_2O_2$	$C_6H_5BrN_2O_2$
M_r	217.03	217.03
Crystal system, space group	Monoclinic, *Pc*	Monoclinic, $P2_1/n$
Temperature (K)	130	130
a, *b*, *c* (Å)	11.1643 (11), 3.8275 (4), 17.2764 (16)	4.4477 (2), 11.4469 (4), 13.8244 (5)
β (°)	98.662 (3)	94.635 (2)
V (Å^3)	729.82 (12)	701.53 (5)
Z	4	4
Radiation type	Mo $K\alpha$	Mo $K\alpha$
μ (mm^{-1})	5.58	5.80
Crystal size (mm)	0.60 × 0.42 × 0.38	0.42 × 0.30 × 0.25
Data collection		
Diffractometer	Bruker D8 Venture Photon II	Bruker D8 Venture Photon II
Absorption correction	Multi-scan (*SADABS*; Krause *et al.*, 2015)	Multi-scan (*SADABS*; Krause *et al.*, 2015)
$T_{\min}$, $T_{\max}$	0.579, 0.746	0.522, 0.746
No. of measured, independent and observed $[I > 2\sigma(I)]$ reflections	12367, 3712, 2965	14025, 2162, 1813
$R_{\rm int}$	0.059	0.035
$(\sin \theta/\lambda)_{\max}$ (Å^{-1})	0.693	0.716
Refinement		
$R[F^2 > 2\sigma(F^2)]$, $wR(F^2)$, S	0.041, 0.080, 1.02	0.023, 0.050, 1.04
No. of reflections	3712	2162
No. of parameters	215	108
No. of restraints	6	2
H-atom treatment	H atoms treated by a mixture of independent and constrained refinement	H atoms treated by a mixture of independent and constrained refinement
$\Delta\rho_{\max}$, $\Delta\rho_{\min}$ (e Å^{-3})	0.51, −0.77	0.54, −0.46
Absolute structure	Flack *x* determined using 1017 quotients $[(I^+) - (I^-)]/[(I^+) + (I^-)]$ (Parsons *et al.*, 2013)	–
Absolute structure parameter	0.030 (12)	–

Computer programs: *APEX3* (Bruker, 2016), *SAINT* (Bruker, 2016), *SHELXT* (Sheldrick, 2015*b*), *SHELXL* (Sheldrick, 2015*a*), *Mercury* (Macrae *et al.*, 2008), *ORTEP-3 for Windows* (Farrugia, 2012), *OLEX2* (Dolomanov *et al.*, 2009) and *publCIF* (Westrip, 2010).

ability of the halogen-bond donor atom, *i.e.* F < Cl < Br < I. Halogen interactions have been found to be very directional, even more so than hydrogen bonds (Metrangolo *et al.*, 2005, 2008). On the other hand, halogen atoms are distinguished by their relatively high electronegativity and are prone to behave as nucleophiles with a tendency to form attractive interactions with electrophilic molecular entities, *e.g.* hydrogen-bond donors (Desiraju *et al.*, 2013). In the case of *meta*-bromonitrobenzene, described by Charlton & Trotter in 1963, short Br⋯C intermolecular contacts were indicated to be significant in the crystal structure stabilization (Charlton & Trotter, 1963). According to calculations (Tsuzuki *et al.*, 2016), the directionality of the halogen–π interactions may be enhanced by introducing an electron-donating substituent to the aromatic ring. We were interested in whether the insertion of a strong electron-donating amine group in the *ortho* or *para* positions towards the Br atom could influence a σ-hole, and thus the interactions with the Ar—Br molecular fragment. According to Mukherjee & Desiraju (2014), the Br atom is worthy of attention because even though much exploitation of halogen and D—H⋯X hydrogen bonds has been carried out, the nature of bromine remains unclear and any study in this area would be useful for future applications, including drug design.

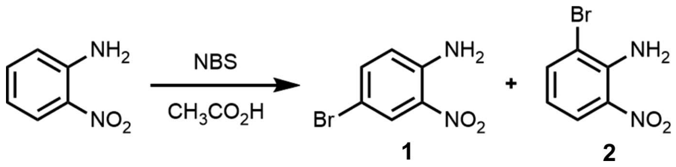

Figure 1
The synthetic procedure for the preparation of **1** and **2**.

2. Experimental

2.1. Synthesis and crystallization

All reagents used were bought from Sigma–Aldrich and used as received without additional purification. ^{1}H NMR spectra were recorded on Bruker Advance III 300 MHz and Agilent NMR 400 MHz DDR2 spectrometers, and chemical shifts were referenced to tetramethylsilane (TMS) using the known chemical shifts of the solvent residual peak.

To a solution of 2-nitroaniline (34.5 g, 0.25 mol) in acetic acid (400 ml), *N*-bromosuccinimide (44.5 g, 0.25 mol) was added portionwise over a period of 30 min at 308–318 K (Fig. 1). The mixture was stirred for 3 h at 318 K, warmed to 363 K and stirred for 2 h. After cooling the mixture to room temperature, it was poured into intensively stirred cold water

(4 l). After 10 min, an orange precipitate was filtered off and washed with water (2 × 200 ml). The obtained crude product was recrystallized from 80% EtOH and dried under vacuum to give pure 4-bromo-2-nitroaniline (yield 39.9 g, 74%) as an orange crystalline solid. From the filtrate, a second crystallization crop was obtained (yield 6.81 g), comprised of 4-bromo-2-nitroaniline and 2-bromo-6-nitroaniline in a 1:0.3 ratio. The NMR spectra are consistent with those published in the literature (Manley *et al.*, 2003; Lemaire *et al.*, 1989).

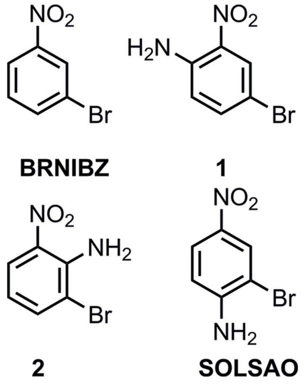

Scheme 1

Analytical data for 4-bromo-2-nitroaniline, ^{1}H NMR (300 MHz, $CDCl_3$): δ 8.26 (*dd*, *J* = 2.3, 0.4 Hz, 1H), 7.42 (*dd*, *J* = 8.9, 2.3 Hz, 1H), 6.73 (*dd*, *J* = 8.9, 0.4 Hz, 1H), 6.10 (*s*, 2H).

Analytical data for 2-bromo-6-nitroaniline, ^{1}H NMR (400 MHz, $CDCl_3$): δ 8.14 (*dd*, *J* = 8.7, 1.5 Hz, 1H), 7.70 (*dd*, *J* = 7.7, 1.5 Hz, 1H), 6.63 (*s*, 2H), 6.62 (*dd*, *J* = 8.7, 7.7 Hz, 1H).

Single crystals of 4-bromo-2-nitroaniline were obtained by slow evaporation from chloroform and of 2-bromo-6-nitroaniline by sublimation of the second crystallization crop under reduced pressure (323 K, 10 mbar; 1 bar = 10^5 Pa).

2.2. Refinement

Crystal data, data collection and structure refinement details are summarized in Table 1. H atoms on C atoms were added to the model at geometrically idealized positions and refined as riding atoms, with $U_{\rm iso}$(H) = 1.2$U_{\rm eq}$(C). H atoms of amino groups were located from a difference Fourier map and refined with restraints on the N—H distances of 0.880 (5) Å.

3. Results and discussion

To investigate the influence of an amino group on interactions with the Br atom in bromonitroanilines, firstly we analyzed the intermolecular interactions in the amino-unsubstituted *meta*-bromonitrobenzene (**BRNIBZ**) crystal structure using Hirshfeld surface (HS) analysis (Spackman & Jayatilaka, 2009). In the original data (Charlton & Trotter, 1963), H-atom positions were not defined, so for further analysis, H atoms were added at neutron-normalized distances using modules implemented in the *Mercury CSD* program (Version 3.10; Macrae *et al.*, 2008). The analysis of the HS indicates that both C—H$\cdots$O$^{\rm i}$ and Br$\cdots\pi^{\rm ii}$ interactions [symmetry codes: (i) $x + 1, y, z - 1$; (ii) $x - \frac{1}{2}, -y + \frac{1}{2}, z - \frac{1}{2}$] are the most important in the stabilization of the crystal structure (Fig. 2*a*). Together, they form layers perpendicular to the longest unit-cell axis *b* (the *a* and *c* axes are four times shorter than *b*). The layers are further joined *via* weak O$\cdots$N$^{\rm iii}$ [symmetry code: (iii) $-x, -y, z + \frac{1}{2}$] contacts between nitro groups (Daszkiewicz, 2013) (Fig. 2*b*). It is noteworthy that a synthon formed exclusively by Br atoms is a zigzag chain propagating along the [101] direction, with a shortest Br$\cdots$C distance of *ca* 3.35 Å and a dihedral angle of ~80° between two consecutive planes defined by the almost flat *m*-bromonitrobenzene molecules. The molecule shows a slight deviation from C_s point-group symmetry described by a Continuous Symmetry Measure (CSM; Zabrodsky *et al.*, 1993) parameter of 0.04 (2) Å (Fig. 2*c*).

The amino group is known to strongly influence the distribution of electron density in aromatic systems, especially in the *ortho* and *para* positions (Hansch *et al.*, 1991). Using a simple reaction procedure, we obtained from *ortho*-nitroaniline two brominated derivatives with an NH_2 group in the *para* and *ortho* positions with respect to the Br atom (Fig. 1). Therefore, two newly characterized isomers are 4-bromo-2-nitroaniline (**1**) and 2-bromo-6-nitroaniline (**2**). In the Cambridge Structural Database (CSD; Version 5.39 of November 2017, plus three updates of November 2017,

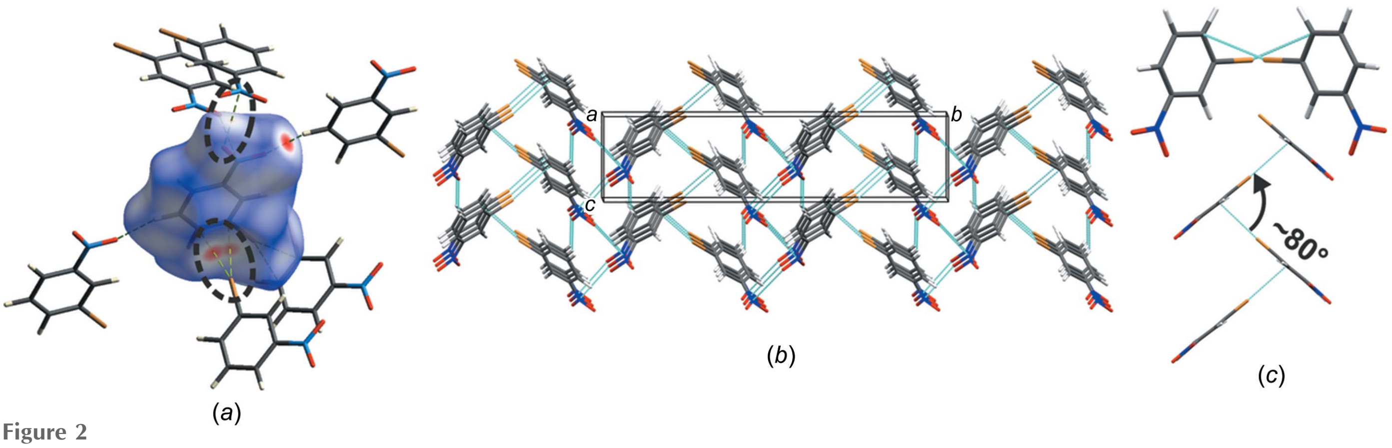

Figure 2
(*a*) The Hirshfeld surface for **BRNIBZ** generated using *CrystalExplorer17* (Turner *et al.*, 2017). (*b*) The intermolecular interactions and packing in the **BRNIBZ** structure. (*c*) The Br$\cdots\pi^{\rm ii}$-bonded chain geometry. [Symmetry code: (ii) $x - \frac{1}{2}, -y + \frac{1}{2}, z - \frac{1}{2}$.]

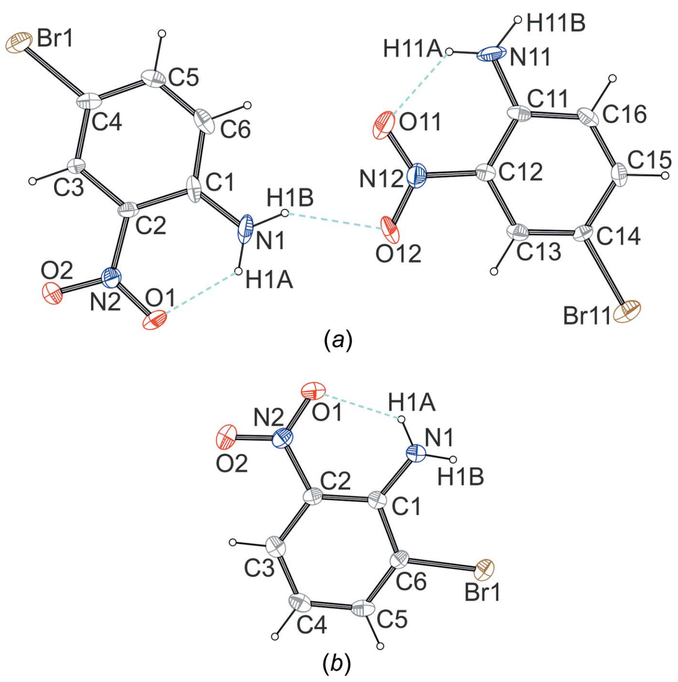

Figure 3
ORTEP-3 (Farrugia, 2012) drawings of (*a*) the two symmetry-independent molecules of **1** and (*b*) a molecule of **2**, with the atom-numbering schemes and hydrogen bonds denoted as dashed lines. Displacement ellipsoids are depicted at the 50% probability level.

Table 2
Hydrogen-bond geometry (Å, °) for **1**.

D—H···*A*	*D*—H	H···*A*	*D*···*A*	*D*—H···*A*
N1—H1*A*···O1	0.89 (6)	1.99 (6)	2.640 (9)	129 (4)
N1—H1*B*···O12^{i}	0.88 (5)	2.19 (7)	2.967 (9)	148 (6)
N11—H11*A*···O1^{ii}	0.88 (3)	2.23 (4)	3.104 (8)	169 (8)
N11—H11*B*···O11	0.88 (6)	1.97 (6)	2.655 (9)	134 (6)
N11—H11*B*···N12	0.88 (6)	2.58 (6)	2.939 (9)	106 (5)

Symmetry codes: (i) $x, y-1, z$; (ii) $x+1, y, z$.

February 2018 and May 2018; Groom *et al.*, 2016), under refcode SOLSAO (Arshad *et al.*, 2009), the crystal structure of a third isomer, 2-bromo-4-nitroaniline, was found. This compound was obtained from *para*-nitroaniline and thus bromination occurred in the *ortho* position with respect to the amino group.

Compound **1** (4-bromo-2-nitroaniline) crystallizes in the polar space group *Pc* with two molecules in an asymmetric unit (denoted **1a** and **1b**; Fig. 3*a*). Both molecules are flat, showing close to C_s point-group symmetry, with CSM parameters of 0.30 (5) and 0.11 (3) Å for **1a** and **1b**, respectively. The differences between the two molecules are small, which can be seen in Fig. 4(*b*), which shows their superposition. In both cases, the nitro and amino groups form intramolecular N—H···O hydrogen bonds (Fig. 3*a* and Table 2), with N···O

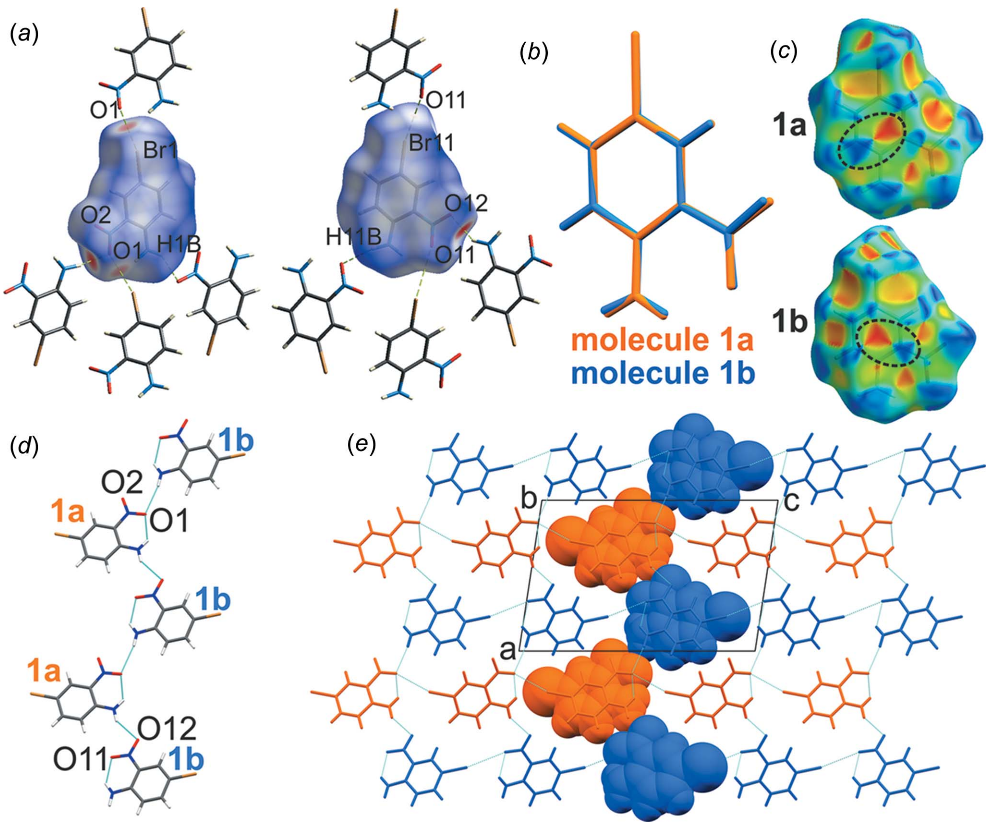

Figure 4
(*a*) The Hirshfeld surfaces for molecules **1a** (left) and **1b** (right). (*b*) An overlay of molecules **1a** (orange) and **1b** (blue). (*c*) Shape index surfaces of both molecules. (*d*) The basic chain motif in the structure built from hydrogen bonds. (*e*) The packing and intermolecular interactions in **1**, with the basic synthon shown in space-filling display style.

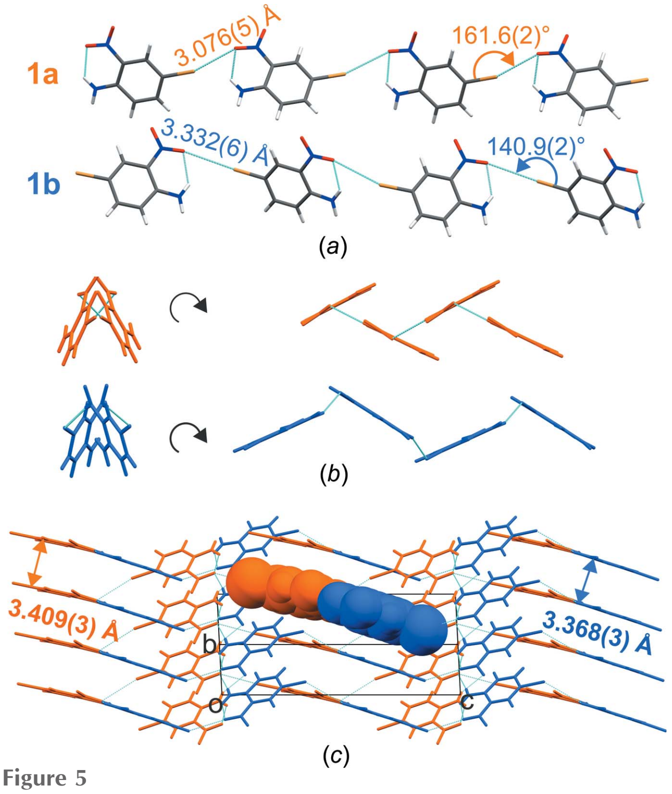

Figure 5
(*a*)/(*b*) The chains formed by both molecules of **1** *via* Br···O halogen bonds. (*c*) Packing diagram with the main N—H···O hydrogen-bonded chain highlighted by spheres of arbitrary radius and with the intermolecular interactions shown as thin dotted lines. The distances between stacked molecules are given.

distances of 2.640 (9) and 2.655 (9) Å for **1a** and **1b**, respectively.

The introduction of the amino substituent provides the possibility of forming 'classical' intermolecular hydrogen bonds. As recognized by the Hirshfeld surface (HS) analysis, the molecules of **1** display relatively strong intermolecular hydrogen bonding between the amino and nitro groups, as well as Br···O halogen bonds (Fig. 4*a*) and π–π stacking interactions (Fig. 4*c*). It is worth noting that C—Br···O interactions have been proven to be typical weak halogen bonds, with a mean Br···O distance of 3.18 Å and a C—Br···O angle of 160°, for intermolecular contacts shorter than the sum of the van der Waals radii and with a tendency to be more linear when the distance shortens (Nayak *et al.*, 2012). Nevertheless, a basic molecular synthon is a chain built of **1a** and **1b** bonded alternately by N—H···O hydrogen bonds (Fig. 4*d* and Table 2). For the **1a** molecule, surprisingly, the less sterically accessible O1 atom is involved in the interaction, while in the **1b** molecule, the hydrogen bond is formed *via* the external O12 atom. The chain is essentially flat as a result of the spatial arrangement of molecules **1a** and **1b**, which are almost coplanar, with twist and fold angles between their planes of 5.9 (2) and 2.1 (2)°, respectively.

Table 3
Hydrogen-bond geometry (Å, °) for **2**.

D—H···*A*	*D*—H	H···*A*	*D*···*A*	*D*—H···*A*
N1—H1*A*···O1	0.88 (1)	1.99 (2)	2.635 (2)	130 (2)
N1—H1*A*···O1$^{\rm i}$	0.88 (1)	2.43 (2)	3.201 (2)	148 (2)
N1—H1*B*···Br1	0.88 (2)	2.57 (2)	3.0432 (15)	115 (2)
C3—H3···O2	0.95	2.33	2.661 (2)	100
C5—H5···O2$^{\rm ii}$	0.95	2.53	3.253 (2)	133

Symmetry codes: (i) $-x, -y+1, -z+1$; (ii) $x+\frac{1}{2}, -y+\frac{3}{2}, z-\frac{1}{2}$.

The observed difference of the topology of the strongest interactions in **1a** and **1b** molecules results in changes in the networks of weak contacts observed for each molecule. With regard to the Hirshfeld surfaces, short Br···O (Fig. 4*a*) and π-stacking interactions (Fig. 4*c*) can be noticed. Therefore, the basic chains are further joined together by two sets of distinguishable Br···O halogen bonds supported by π-stacking interactions, both of which are formed selectively between molecules of one kind (Fig. 5). Molecules **1a** form halogen bonds with a distance between the donor (Br1) and acceptor (O1) of 3.076 (5) Å and a C4—Br1···O1$^{\rm iii}$ angle of 161.6 (2)° [symmetry code: (iii) $x, -y+2, z-\frac{1}{2}$], while molecules **1b** are more distant, with a Br11···O11$^{\rm iv}$ distance of 3.332 (5) Å and a C14—Br11···O11$^{\rm iv}$ angle of 140.9 (2)° [symmetry code: (iv) $x, -y+2, z+\frac{1}{2}$]. As a result, each molecule forms a halogen-bonded chain stretching along the *c* axis, but with a reverse direction of the donor–acceptor sequence. Although the topologies of those subnetworks are the same, the shapes of the chains differ significantly (Figs. 5*a* and 5*b*).

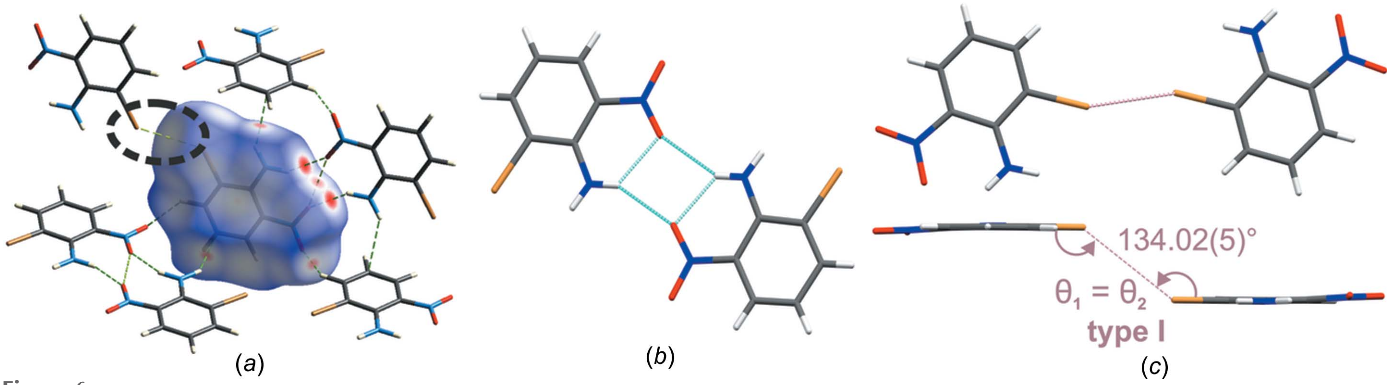

Figure 6
(*a*) The Hirshfeld surface of molecule **2**, with weak Br···Br contacts marked. (*b*) The basic dimeric N—H···O hydrogen-bonded synthon. (*c*) The dimer formed by Br···Br interactions.

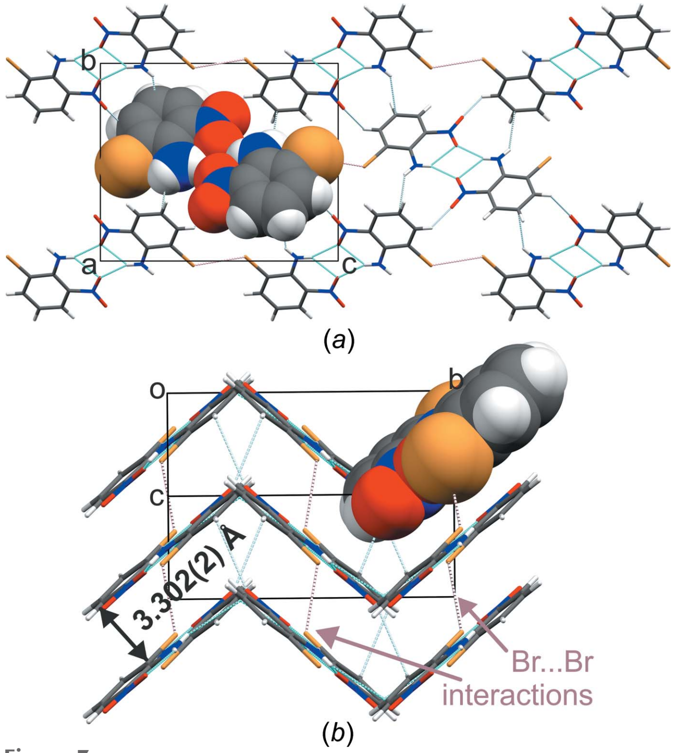

Figure 7
The packing and intermolecular interactions in **2**, with the basic dimeric motif depicted in space-filling style, viewed (*a*) along [100] and (*b*) along [10$\overline{1}$].

In the halogen-bonded chain in **1a**, the distance between the molecular planes of alternate molecules is ~3.52 Å, while the analogous distance in the **1b** chain is ~5.36 Å. This is a result of the different orientation of the molecules towards the (110) crystallographic plane, that is, the dihedral angles between the planes of the molecules and the (110) crystallographic plane are ~12.91 and ~18.33° for the **1a** and **1b** chains, respectively. In effect, the Br···O chains of **1a** and **1b** can be described as herringbone and zigzag arrangements, respectively (Fig. 5*b*). A more relaxed molecular arrangement in the latter chain promotes π-stacking interactions between **1b** molecules related by translation along the [010] direction. Indeed, at the expense of the weakening of the Br···O interactions, a shortening of the π–π distance is observed, from 3.409 (3) Å in **1a** to 3.368 (3) Å in **1b** (measured as the distance between molecular planes) (Fig. 5*c*). The relevance of the stacking interactions in the crystal structure stabilization can be confirmed by the presence of red and blue complementary triangles on the shape index surfaces (McKinnon *et al.*, 2004) (Fig. 4*c*).

Isomeric compound **2** (2-bromo-6-nitroaniline) crystallizes in the centrosymmetric space group $P2_1/n$, with one molecule in the asymmetric unit. The whole molecule is essentially flat, with a CSM parameter of 0.15 (4) Å, describing a deviation from C_s point-group symmetry. Similar to **1**, an intramolecular N1—H1*A*···O1 hydrogen bond (Table 3) is formed between the amino and nitro groups. In addition, in **2**, the second amine H atom (H1*B*) is in close proximity to the Br atom, with an N···Br distance of 3.043 (2) Å, enabling the formation of a weak intramolecular interaction. In **2**, intermolecular N1—H1*A*···O1^{i} [symmetry code: (i) $-x, -y+1, -z+1$] hydrogen bonds between neighbouring molecules lead to a basic dimeric motif (Fig. 6*b*). A linkage within this molecular synthon is additionally supported by a close O···O contact visible on the Hirshfeld surfaces (Fig. 6*a*).

Dimers further interact with each other *via* weak C5—H5···O2^{ii} [symmetry code: (ii) $x+\frac{1}{2}, -y+\frac{3}{2}, z-\frac{1}{2}$] hydrogen bonds supported by N2—H2*B*···π^{iii} [symmetry code: (iii) $-x+\frac{1}{2}, y-\frac{1}{2}, -z+\frac{1}{2}$] contacts, forming a zigzag cross-section layer parallel to the (10$\overline{1}$) crystallographic plane, within which the molecular planes are almost perpendicular (Fig. 7). The layers are linked together by weak stacking interactions [π–π distance of 3.302 (2) Å] supported by weak Br···Br contacts. Halogen interactions in this structure are very weak and thus barely noticeable on the Hirshfeld surface (Fig. 6*a*). The distance between the bromine substituents is 3.5821 (5) Å, with a C6—Br1···Br1^{iv} [symmetry code: (iv) $-x, -y+1, -z$] angle of 134.02 (5)°. The geometry of this contact is in agreement with that of the postulated type I halogen–halogen bonds (Mukherjee & Desiraju, 2014) (Fig. 6*c*).

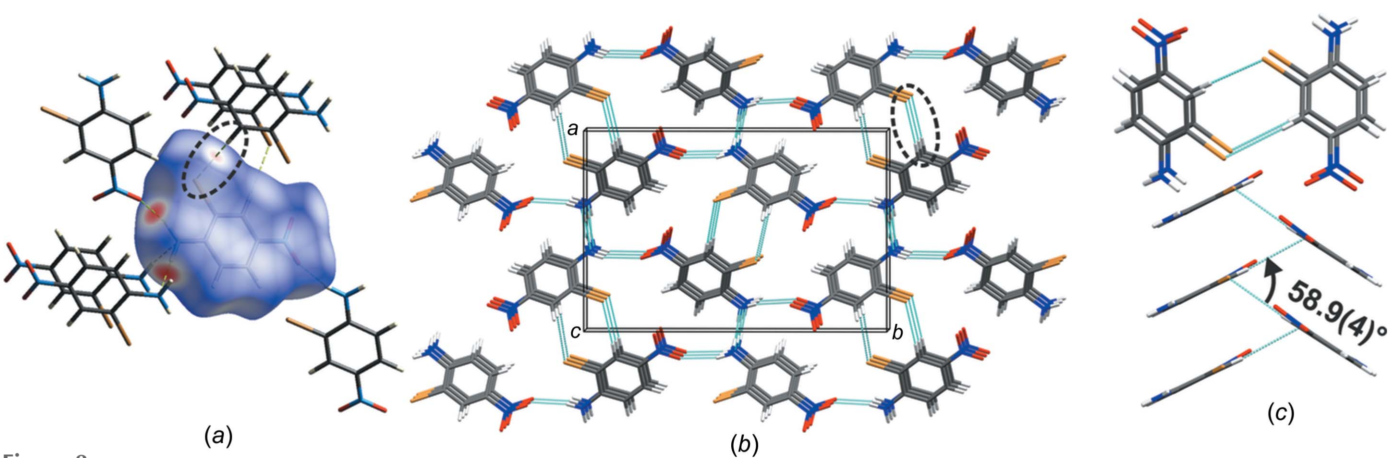

Figure 8
(*a*) Hirshfeld surface for the SOLSAO molecule (Arshad *et al.*, 2009). (*b*) The packing and interactions in the SOLSAO crystal structure and (*c*) the geometry of the chains formed *via* weak C—H···Br interactions.

The structure of a third isomer, with the bromine substituent located in the *ortho* position with respect to the amino group, *i.e.* 2-bromo-4-nitroaniline, has been deposited in the CSD under refcode SOLSAO (Arshad *et al.*, 2009). Nevertheless, the packing arrangement and intermolecular interactions have not been thoroughly investigated, despite the fact that this compound crystallizes in the polar space group $Pna2_1$ and, together with **1**, may be a potential material with nonlinear optical properties (Nalwa *et al.*, 1997). Similar to the other isomers, the SOLSAO molecule is essentially flat, with a CSM parameter describing the deviation from C_s point-group symmetry of 0.12 (3) Å. In this case, an intramolecular N1—H2···Br1 hydrogen bond is observed, with H···Br, N···Br and N—H···Br parameters of 2.68 Å, 3.095 (5) Å and 111°, respectively. Analysis of the HS (Fig. 8*a*) confirms that the N1—H2···O1^{i} [H···O = 2.32 Å, N···O = 3.049 (7) Å and N—H···O = 143°; symmetry code: (i) $-x+\frac{1}{2}, y+\frac{1}{2}, z+\frac{1}{2}$] and N1—H1···N1^{ii} [H···N = 2.32 Å, N···N = 3.158 (7) Å and N—H···N = 167°; symmetry code: (ii) $-x, -y+1, z+\frac{1}{2}$] hydrogen bonds form a three-dimensional network stabilizing the crystal structure. However, much weaker C2—H3···Br1^{iii} [H···Br = 2.97 Å, C···Br = 3.899 (5) Å and C—H···Br = 177°; symmetry code: (iii) $-x+1, -y+1, z-\frac{1}{2}$] hydrogen bonds can be found auxiliary to 'classical' hydrogen bonds (Fig. 8*b*). A subnetwork formed solely of C—H···Br interactions is a herringbone chain of $p2_1$ rod group symmetry (Kopský & Litvin, 2006), extending along the [001] direction, with angles between the molecular planes close to 60° (Fig. 8*c*).

It is worth underlining that all the above-mentioned halogen or hydrogen-bond interactions with the Br atom are strongly directional. This feature is clearly depicted on the resolved HS fingerprint plots of the atoms (Spackman & McKinnon, 2002) shown in Fig. 9(*a*). The characteristic whiskers in the case of the Br···O and Br···Br halogen bonds, as well as on the map for H···Br contacts, can be noticed. Also, the short Br···C contacts are meaningful, with a surface coverage of 8.1%. What is more, all the scrutinized intermolecular interactions with the Br atom show the bonding character as revealed by a Reduced Density Gradient NonCovalent Interactions (RDG NCI) analysis (Johnson *et*

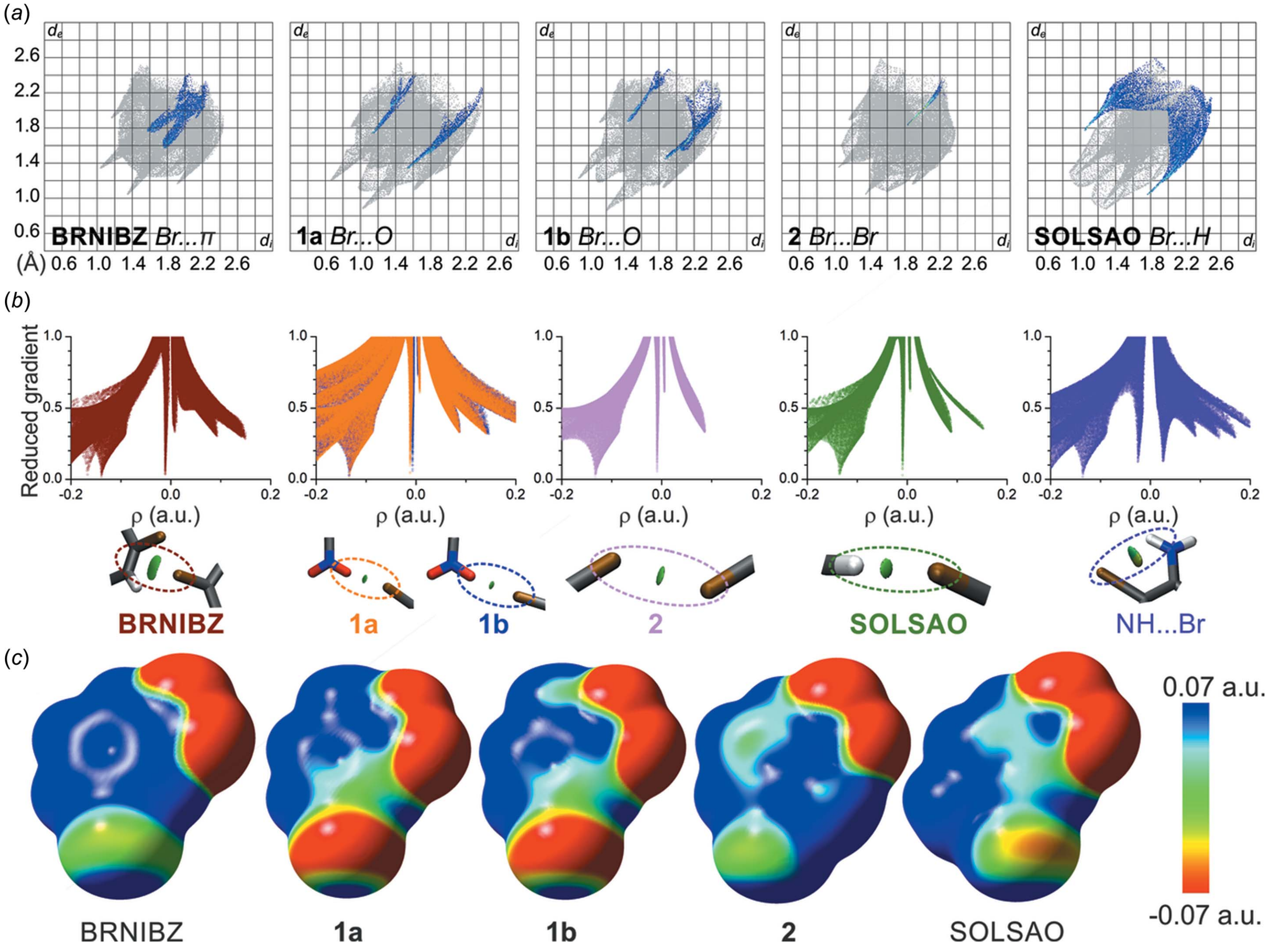

Figure 9

(*a*) Atom-type-resolved HS fingerprint plots for weak interactions with the Br atom. (*b*) Reduced Density Gradient NCI plots for selected interactions. (*c*) Electrostatic potential surfaces (EPS) for the analyzed molecules. The isovalue of all surfaces was set at 0.02.

al., 2010). In the plots shown in Fig. 9(*b*), negative low-density low-gradient peaks are observed. What is worth noting is that the RDG NCI method additionally confirms the energy difference between the Br···O interactions formed by molecules **1a** and **1b** (Fig. 9*b*, second from left), as the B11···O11 (**1b**) spike corresponds to the interaction of less stabilizing character (blue).

In addition, for the crystal structures of **2** and SOLSAO, the bonding nature of the subtle intramolecular N—H···Br contacts was confirmed by the RDG NCI analysis (Fig. 9*b*, most on the right). Their importance is also revealed when analyzing the electrostatic potential surfaces (EPS, Fig. 9*c*), generated using molecular geometries from crystal structures with H-atom positions normalized to the neutronic distances (the calculations were performed at the DFT b97d3/aug-cc-pvtz level of theory using the *GAUSSIAN09* program; Frisch *et al.*, 2009). In **2** and SOLSAO, a local depletion of the negative values on the bromine substituent in the neighbourhood of the NH_2 group can be noticed. Thus, in these cases, some of the additional charge density transferred as a result of the mesomeric effect is donated back to the NH_2 substituent. Nevertheless, in both structures, the Br atom acts as a nucleophile in halogen and hydrogen bonds, respectively. Generally, on all surfaces, a local enrichment of the negative electrostatic potential value in the vicinity of the bromine substituent is observed while the outermost part of the atom surface is positive. The σ-hole electrostatic potential distribution is particularly visible in the case of the **1a**, **1b** and **BRNIBZ** molecules. Yet, in the latter, the charge difference between the electrophilic and nucleophilic regions of the Br atom are not as pronounced as in **1** due to the lack of additional electron density provided by the amino group.

4. Summary

The series of structures of *meta*-bromonitrobenzene and its NH_2-substituted derivatives was studied with special attention being paid to the nature of the halogen-atom interactions. The compounds were selected according to the possibility of inducing a strong mesomeric effect by the amino group, and thus observing a strong influence on electron charge distribution over the molecule. The crystal structure of *meta*-bromonitrobenzene (**BRNIBZ**) is stabilized by weak interactions only and the bromine substituent plays a crucial role by interacting as a strong electrophile with the π electrons of a neighbouring molecule. When the amino group is introduced *para* to Br (*i.e.* in **1**), the electrophilic character of the Br atom is sustained and intermolecular Br···O interactions are formed. They play an important role in the stabilization of the crystal structure, as they are involved in linking the basic N—H···O hydrogen-bonded chain motifs in the three-dimensional structure. In the case of compound **2**, with the amino group *ortho* to both the Br and NO_2 substituents, the interactions with the Br atom are of a binary character, that is, the Br atom acts a nucleophile in a subtle intramolecular C—H···Br hydrogen bonding, as well as forming Br···Br halogen bonds in which the electrophilic nature of the σ-hole is manifested. In the SOLSAO structure, with the amino group *ortho* with respect to Br, the bromine substituent plays the role of an acceptor in C—H···Br hydrogen bonds (both intra- and intermolecular), which distinguishes this structure from the former isomers, since Br plays the role of a nucleophile exclusively. Additionally, electrostatic potential surfaces were analyzed and the observed specific 'switch' of the Br atom role in the intermolecular interactions was linked to modifications of the electron-density distribution in the aromatic ring caused by the electron-donating amino group located in the most activated *ortho* and *para* positions relative to the Br atom. It was shown that well-known electronic effects not only influence the electron distribution in the molecule, but can also allow the engineering of various intermolecular interactions with halogens. We believe that other simple aromatic halide derivatives with strong electron-donating/withdrawing groups are worth investigating.

Acknowledgements

PHM acknowledges the Operational Project Knowledge Education Development 2014–2020 cofinanced by the European Social Fund. The X-ray structures were determined in the Advanced Crystal Engineering Laboratory (aceLAB) at the Chemistry Department of the University of Warsaw.

Funding information

Funding for this research was provided by: Faculty of Chemistry, Warsaw University of Technology.

References

Arshad, M. N., Tahir, M. N., Khan, I. U. & Shafiq, M. (2009). *Acta Cryst.* E**65**, o480.

Brinck, T., Murray, J. S. & Politzer, P. (1992). *Int. J. Quantum Chem.* **44**, 57–64.

Bruker (2016). *APEX3* and *SAINT*. Bruker AXS Inc., Madison, Wisconsin, USA.

Cavallo, G., Metrangolo, P., Milani, R., Pilati, T., Priimagi, A., Resnati, G. & Terraneo, G. (2016). *Chem. Rev.* **116**, 2478–2601.

Charlton, T. L. & Trotter, J. (1963). *Acta Cryst.* **16**, 313.

Clark, T., Hennemann, M., Murray, J. S. & Politzer, P. (2007). *J. Mol. Model.* **13**, 291–296.

Daszkiewicz, M. (2013). *CrystEngComm*, **15**, 10427–10430.

Desiraju, G. R., Ho, P. S., Kloo, L., Legon, A. C., Marquardt, R., Metrangolo, P., Politzer, P., Resnati, G. & Rissanen, K. (2013). *Pure Appl. Chem.* **85**, 1711–1713.

Dolomanov, O. V., Bourhis, L. J., Gildea, R. J., Howard, J. A. K. & Puschmann, H. (2009). *J. Appl. Cryst.* **42**, 339–341.

Farrugia, L. J. (2012). *J. Appl. Cryst.* **45**, 849–854.

Frisch, M. J., *et al.* (2009). *GAUSSIAN09*. Gaussian Inc., Wallingford, CT, USA. http://www.gaussian.com.

Groom, C. R., Bruno, I. J., Lightfoot, M. P. & Ward, S. C. (2016). *Acta Cryst.* B**72**, 171–179.

Hansch, C., Leo, A. & Taft, R. W. (1991). *Chem. Rev.* **91**, 165–195.

Hussain, I., Capricho, J. & Yawer, M. A. (2016). *Adv. Synth. Catal.* **358**, 3320–3349.

Johnson, E. R., Keinan, S., Mori-Sánchez, P., Contreras-García, J., Cohen, A. J. & Yang, W. (2010). *J. Am. Chem. Soc.* **132**, 6498–6506.

Kopský, V. & Litvin, D. B. (2006). *International Tables for Crystallography*, Vol. E, *Subperiodic Groups*, pp. 37–217. Dordrecht: Springer.

Krause, L., Herbst-Irmer, R., Sheldrick, G. M. & Stalke, D. (2015). *J. Appl. Cryst.* **48**, 3–10.

Lemaire, M., Guy, A., Boutin, P. & Guette, J. P. (1989). *Synthesis*, pp. 761–763.

Macrae, C. F., Bruno, I. J., Chisholm, J. A., Edgington, P. R., McCabe, P., Pidcock, E., Rodriguez-Monge, L., Taylor, R., van de Streek, J. & Wood, P. A. (2008). *J. Appl. Cryst.* **41**, 466–470.

Manley, P. W., Acemoglu, M., Marterer, W. & Pachinger, W. (2003). *Org. Process Res. Dev.* **7**, 436–445.

Matter, H., Nazaré, M., Güssregen, S., Will, D. W., Schreuder, H., Bauer, A., Urmann, M., Ritter, K., Wagner, M. & Wehner, V. (2008). *Angew. Chem. Int. Ed.* **48**, 2911–2916.

McKinnon, J. J., Spackman, M. A. & Mitchell, A. S. (2004). *Acta Cryst.* B**60**, 627–668.

Metrangolo, P., Meyer, F., Pilati, T., Resnati, G. & Terraneo, G. (2008). *Angew. Chem. Int. Ed.* **47**, 6114–6127.

Metrangolo, P., Neukirch, H., Pilati, T. & Resnati, G. (2005). *Acc. Chem. Res.* **38**, 386–395.

Mukherjee, A. & Desiraju, G. R. (2014). *IUCrJ*, **1**, 49–60.

Nalwa, H. S., Watanabe, T. & Miyata, S. (1997). *Nonlinear Optics of Organic Molecules and Polymers*, edited by Nalwa, H. S. & Miyata, S., pp. 89–329. Boca Raton: CRC Press.

Nayak, S. K., Terraneo, G., Forni, A., Metrangolo, P. & Resnati, G. (2012). *CrystEngComm*, **14**, 4259–4261.

Parsons, S., Flack, H. D. & Wagner, T. (2013). *Acta Cryst.* B**69**, 249–259.

Sheldrick, G. M. (2015*a*). *Acta Cryst.* C**71**, 3–8.

Sheldrick, G. M. (2015*b*). *Acta Cryst.* A**71**, 3–8.

Spackman, M. A. & Jayatilaka, D. (2009). *CrystEngComm*, **11**, 19–32.

Spackman, M. A. & McKinnon, J. J. (2002). *CrystEngComm*, **4**, 378–392.

Sun, H., Horatscheck, A., Martos, V., Bartetzko, M., Uhrig, U., Lentz, D., Schmieder, P. & Nazaré, M. (2017). *Angew. Chem. Int. Ed.* **56**, 6454–6458.

Tian, M., Cui, X., Yuan, M., Yang, J., Ma, J. & Dong, Z. (2017). *Green Chem.* **19**, 1548–1554.

Tsuzuki, S., Uchimaru, T., Wakisaka, A. & Ono, T. (2016). *J. Phys. Chem. A*, **120**, 7020–7029.

Turner, M. J., McKinnon, J. J., Wolff, S. K., Grimwood, D. J., Spackman, P. R., Jayatilaka, D. & Spackman, M. A. (2017). *CrystalExplorer17*. University of Western Australia.

Westrip, S. P. (2010). *J. Appl. Cryst.* **43**, 920–925.

Zabrodsky, H., Peleg, S. & Avnir, D. (1993). *J. Am. Chem. Soc.* **115**, 8278–8289.

supporting information

Acta Cryst. (2018). C**74** [https://doi.org/10.1107/S2053229618013608]

The study of interactions with a halogen atom: influence of NH_2 group insertion on the crystal structures of *meta*-bromonitrobenzene derivatives

Paulina H. Marek, Mateusz Urban and Izabela D. Madura

Computing details

For both structures, data collection: *APEX3* (Bruker, 2016); cell refinement: *SAINT* (Bruker, 2016); data reduction: *SAINT* (Bruker, 2016); program(s) used to solve structure: *SHELXT* (Sheldrick, 2015*b*); program(s) used to refine structure: *SHELXL* (Sheldrick, 2015*a*); molecular graphics: *Mercury CSD* (Macrae *et al.*, 2008) and *ORTEP-3 for Windows* (Farrugia, 2012); software used to prepare material for publication: OLEX2 (Dolomanov *et al.*, 2009) and *publCIF* (Westrip, 2010).

4-Bromo-2-nitroaniline (1)

Crystal data

$C_6H_5BrN_2O_2$
$M_r = 217.03$
Monoclinic, *Pc*
$a = 11.1643\ (11)$ Å
$b = 3.8275\ (4)$ Å
$c = 17.2764\ (16)$ Å
$\beta = 98.662\ (3)°$
$V = 729.82\ (12)$ Å^3
$Z = 4$
$F(000) = 424$
$D_x = 1.975$ Mg m^{-3}
Mo $K\alpha$ radiation, $\lambda = 0.71073$ Å
Cell parameters from 3126 reflections
$\theta = 2.4–27.6°$
$\mu = 5.58$ mm^{-1}
$T = 130$ K
Needle, yellow
0.60 × 0.42 × 0.38 mm

Data collection

Bruker D8 Venture Photon II diffractometer
Radiation source: TRIUMPH monochromator and fine focus sealed tube
φ and ω scans
Absorption correction: multi-scan (SADABS; Krause *et al.*, 2015)
$T_{min} = 0.579$, $T_{max} = 0.746$
12367 measured reflections
3712 independent reflections
2965 reflections with $I > 2\sigma(I)$
$R_{int} = 0.059$
$\theta_{max} = 29.5°$, $\theta_{min} = 2.4°$
$h = -15 \rightarrow 15$
$k = -5 \rightarrow 5$
$l = -23 \rightarrow 20$

Refinement

Refinement on F^2
Least-squares matrix: full
$R[F^2 > 2\sigma(F^2)] = 0.041$
$wR(F^2) = 0.080$
$S = 1.02$
3712 reflections
215 parameters
6 restraints
Primary atom site location: dual
Hydrogen site location: mixed
H atoms treated by a mixture of independent and constrained refinement
$w = 1/[\sigma^2(F_o^2)]$
where $P = (F_o^2 + 2F_c^2)/3$
$(\Delta/\sigma)_{max} < 0.001$
$\Delta\rho_{max} = 0.51$ e Å^{-3}
$\Delta\rho_{min} = -0.77$ e Å^{-3}

Absolute structure: Flack *x* determined using 1017 quotients [(I+)-(I-)]/[(I+)+(I-)] (Parsons *et al.*, 2013)
Absolute structure parameter: 0.030 (12)

Special details

Geometry. All esds (except the esd in the dihedral angle between two l.s. planes) are estimated using the full covariance matrix. The cell esds are taken into account individually in the estimation of esds in distances, angles and torsion angles; correlations between esds in cell parameters are only used when they are defined by crystal symmetry. An approximate (isotropic) treatment of cell esds is used for estimating esds involving l.s. planes.

Fractional atomic coordinates and isotropic or equivalent isotropic displacement parameters (Å^2)

	x	*y*	*z*	U_{iso}*/U_{eq}
Br1	0.27039 (4)	0.95174 (18)	0.14819 (3)	0.0270 (2)
O1	0.1481 (4)	0.7273 (14)	0.4930 (3)	0.0280 (12)
O2	0.0525 (4)	1.0151 (13)	0.3946 (3)	0.0312 (12)
N1	0.3685 (7)	0.4902 (15)	0.4868 (4)	0.0277 (16)
H1A	0.313 (5)	0.521 (16)	0.518 (3)	0.018 (18)*
H1B	0.440 (3)	0.40 (2)	0.504 (5)	0.04 (2)*
N2	0.1407 (5)	0.8386 (15)	0.4244 (3)	0.0208 (12)
C1	0.3445 (6)	0.6017 (18)	0.4122 (4)	0.0196 (14)
C2	0.2357 (6)	0.7667 (18)	0.3791 (4)	0.0165 (13)
C3	0.2143 (6)	0.8733 (15)	0.3005 (3)	0.0143 (12)
H3	0.1404	0.9844	0.2797	0.017*
C4	0.3009 (6)	0.8151 (17)	0.2546 (4)	0.0192 (14)
C5	0.4104 (6)	0.6541 (18)	0.2851 (4)	0.0210 (15)
H5	0.4699	0.6126	0.2523	0.025*
C6	0.4319 (6)	0.5560 (18)	0.3623 (4)	0.0250 (15)
H6	0.5079	0.4547	0.3826	0.030*
Br11	0.77175 (6)	0.51283 (17)	0.85196 (4)	0.0268 (2)
O11	0.6691 (5)	1.1576 (16)	0.5080 (3)	0.0378 (14)
O12	0.5605 (4)	1.1624 (16)	0.6013 (3)	0.0387 (14)
N11	0.8927 (6)	0.9025 (18)	0.5326 (4)	0.0291 (14)
H11A	0.969 (2)	0.86 (2)	0.528 (5)	0.04 (2)*
H11B	0.837 (5)	1.016 (18)	0.501 (4)	0.04 (3)*
N12	0.6553 (5)	1.0795 (16)	0.5758 (4)	0.0254 (14)
C11	0.8602 (6)	0.8231 (17)	0.6033 (4)	0.0187 (14)
C12	0.7478 (6)	0.9009 (16)	0.6259 (4)	0.0172 (13)
C13	0.7217 (6)	0.8121 (17)	0.7007 (4)	0.0179 (14)
H13	0.6451	0.8691	0.7149	0.022*
C14	0.8055 (6)	0.6462 (16)	0.7522 (4)	0.0159 (13)
C15	0.9211 (6)	0.5656 (16)	0.7317 (4)	0.0196 (13)
H15	0.9808	0.4539	0.7684	0.024*
C16	0.9454 (6)	0.6492 (17)	0.6595 (4)	0.0199 (14)
H16	1.0223	0.5894	0.6460	0.024*

Atomic displacement parameters (Å^2)

	U^{11}	U^{22}	U^{33}	U^{12}	U^{13}	U^{23}
Br1	0.0404 (5)	0.0233 (3)	0.0199 (4)	0.0028 (4)	0.0134 (4)	0.0035 (4)
O1	0.029 (3)	0.043 (3)	0.012 (3)	0.003 (2)	0.007 (2)	0.004 (2)
O2	0.019 (2)	0.050 (4)	0.025 (3)	0.013 (2)	0.005 (2)	0.009 (2)
N1	0.030 (4)	0.029 (4)	0.020 (3)	0.009 (3)	−0.007 (3)	0.006 (3)
N2	0.014 (3)	0.031 (3)	0.017 (3)	−0.001 (2)	0.000 (2)	0.002 (2)
C1	0.015 (3)	0.016 (3)	0.025 (4)	0.002 (3)	−0.007 (3)	0.001 (3)
C2	0.015 (3)	0.022 (4)	0.013 (3)	−0.003 (3)	0.005 (2)	−0.001 (3)
C3	0.014 (3)	0.018 (3)	0.012 (3)	0.000 (2)	0.004 (3)	0.001 (2)
C4	0.021 (4)	0.020 (3)	0.018 (4)	−0.005 (3)	0.009 (3)	−0.003 (3)
C5	0.016 (3)	0.023 (4)	0.025 (4)	−0.002 (3)	0.008 (3)	−0.002 (3)
C6	0.013 (3)	0.028 (4)	0.032 (4)	0.004 (3)	0.000 (3)	−0.001 (3)
Br11	0.0406 (5)	0.0233 (3)	0.0179 (4)	−0.0007 (3)	0.0091 (3)	0.0024 (3)
O11	0.036 (3)	0.054 (4)	0.022 (3)	0.003 (3)	−0.001 (3)	0.015 (3)
O12	0.014 (3)	0.061 (4)	0.040 (3)	0.014 (2)	0.001 (2)	0.015 (3)
N11	0.030 (4)	0.042 (4)	0.018 (3)	−0.004 (3)	0.015 (3)	−0.001 (3)
N12	0.020 (3)	0.032 (3)	0.023 (3)	−0.001 (3)	−0.001 (3)	0.008 (3)
C11	0.020 (4)	0.018 (4)	0.020 (4)	0.001 (3)	0.009 (3)	−0.005 (3)
C12	0.016 (3)	0.019 (3)	0.018 (3)	0.001 (3)	0.005 (3)	−0.002 (2)
C13	0.015 (3)	0.019 (3)	0.022 (4)	−0.001 (3)	0.008 (3)	0.001 (3)
C14	0.020 (3)	0.016 (3)	0.013 (3)	−0.001 (3)	0.004 (3)	0.002 (2)
C15	0.016 (3)	0.021 (3)	0.020 (3)	0.004 (3)	−0.004 (3)	0.000 (3)
C16	0.013 (3)	0.023 (3)	0.025 (4)	0.003 (3)	0.005 (3)	−0.004 (3)

Geometric parameters (Å, º)

Br1—C4	1.892 (7)	Br11—C14	1.890 (6)
O1—N2	1.249 (6)	O11—N12	1.240 (8)
O2—N2	1.241 (7)	O12—N12	1.247 (7)
N1—H1A	0.879 (7)	N11—H11A	0.881 (7)
N1—H1B	0.879 (7)	N11—H11B	0.880 (7)
N1—C1	1.346 (10)	N11—C11	1.360 (9)
N2—C2	1.436 (8)	N12—C12	1.419 (9)
C1—C2	1.411 (9)	C11—C12	1.401 (9)
C1—C6	1.407 (10)	C11—C16	1.419 (9)
C2—C3	1.405 (8)	C12—C13	1.409 (9)
C3—H3	0.9500	C13—H13	0.9500
C3—C4	1.358 (8)	C13—C14	1.348 (9)
C4—C5	1.399 (9)	C14—C15	1.421 (9)
C5—H5	0.9500	C15—H15	0.9500
C5—C6	1.370 (10)	C15—C16	1.355 (9)
C6—H6	0.9500	C16—H16	0.9500
H1A—N1—H1B	122 (7)	H11A—N11—H11B	130 (8)
C1—N1—H1A	119 (5)	C11—N11—H11A	115 (5)
C1—N1—H1B	119 (6)	C11—N11—H11B	115 (6)

O1—N2—C2	120.2 (5)	O11—N12—O12	120.3 (6)
O2—N2—O1	120.9 (5)	O11—N12—C12	120.6 (6)
O2—N2—C2	118.9 (5)	O12—N12—C12	119.0 (6)
N1—C1—C2	124.3 (7)	N11—C11—C12	125.1 (6)
N1—C1—C6	119.4 (6)	N11—C11—C16	118.5 (6)
C6—C1—C2	116.3 (6)	C12—C11—C16	116.4 (6)
C1—C2—N2	121.8 (6)	C11—C12—N12	122.1 (6)
C3—C2—N2	116.1 (6)	C11—C12—C13	121.5 (6)
C3—C2—C1	122.1 (6)	C13—C12—N12	116.4 (5)
C2—C3—H3	120.5	C12—C13—H13	120.0
C4—C3—C2	119.1 (6)	C14—C13—C12	120.0 (6)
C4—C3—H3	120.5	C14—C13—H13	120.0
C3—C4—Br1	118.8 (5)	C13—C14—Br11	121.0 (5)
C3—C4—C5	120.7 (6)	C13—C14—C15	120.3 (6)
C5—C4—Br1	120.5 (5)	C15—C14—Br11	118.8 (5)
C4—C5—H5	119.9	C14—C15—H15	120.2
C6—C5—C4	120.2 (6)	C16—C15—C14	119.6 (6)
C6—C5—H5	119.9	C16—C15—H15	120.2
C1—C6—H6	119.2	C11—C16—H16	118.9
C5—C6—C1	121.7 (6)	C15—C16—C11	122.3 (6)
C5—C6—H6	119.2	C15—C16—H16	118.9

Br1—C4—C5—C6	179.9 (5)	Br11—C14—C15—C16	177.9 (5)
O1—N2—C2—C1	−6.5 (10)	O11—N12—C12—C11	3.7 (10)
O1—N2—C2—C3	174.2 (6)	O11—N12—C12—C13	−177.7 (6)
O2—N2—C2—C1	172.8 (6)	O12—N12—C12—C11	−175.1 (6)
O2—N2—C2—C3	−6.6 (9)	O12—N12—C12—C13	3.6 (9)
N1—C1—C2—N2	1.7 (11)	N11—C11—C12—N12	−0.8 (10)
N1—C1—C2—C3	−179.0 (6)	N11—C11—C12—C13	−179.4 (7)
N1—C1—C6—C5	177.7 (7)	N11—C11—C16—C15	178.9 (7)
N2—C2—C3—C4	179.5 (6)	N12—C12—C13—C14	−179.1 (6)
C1—C2—C3—C4	0.2 (10)	C11—C12—C13—C14	−0.5 (10)
C2—C1—C6—C5	−2.5 (10)	C12—C11—C16—C15	−0.8 (10)
C2—C3—C4—Br1	178.9 (5)	C12—C13—C14—Br11	−178.3 (5)
C2—C3—C4—C5	−0.5 (9)	C12—C13—C14—C15	1.1 (10)
C3—C4—C5—C6	−0.7 (10)	C13—C14—C15—C16	−1.6 (10)
C4—C5—C6—C1	2.2 (10)	C14—C15—C16—C11	1.4 (10)
C6—C1—C2—N2	−178.0 (6)	C16—C11—C12—N12	178.9 (6)
C6—C1—C2—C3	1.3 (10)	C16—C11—C12—C13	0.3 (9)

Hydrogen-bond geometry (Å, º)

D—H···*A*	*D*—H	H···*A*	*D*···*A*	*D*—H···*A*
N1—H1*A*···O1	0.89 (6)	1.99 (6)	2.640 (9)	129 (4)
N1—H1*B*···O12^{i}	0.88 (5)	2.19 (7)	2.967 (9)	148 (6)
N11—H11*A*···O1^{ii}	0.88 (3)	2.23 (4)	3.104 (8)	169 (8)

N11—H11*B*···O11	0.88 (6)	1.97 (6)	2.655 (9)	134 (6)
N11—H11*B*···N12	0.88 (6)	2.58 (6)	2.939 (9)	106 (5)

Symmetry codes: (i) *x*, *y*−1, *z*; (ii) *x*+1, *y*, *z*.

2-Bromo-6-nitroaniline (2)

Crystal data

$C_6H_5BrN_2O_2$	$F(000) = 424$
$M_r = 217.03$	$D_x = 2.055$ Mg m^{-3}
Monoclinic, $P2_1/n$	Mo $K\alpha$ radiation, $\lambda = 0.71073$ Å
$a = 4.4477$ (2) Å	Cell parameters from 5872 reflections
$b = 11.4469$ (4) Å	$\theta = 2.3$–30.4°
$c = 13.8244$ (5) Å	$\mu = 5.80$ mm^{-1}
$\beta = 94.635$ (2)°	$T = 130$ K
$V = 701.53$ (5) Å^3	Needle, yellow
$Z = 4$	0.42 × 0.30 × 0.25 mm

Data collection

Bruker D8 Venture Photon II diffractometer	2162 independent reflections
φ and ω scans	1813 reflections with $I > 2\sigma(I)$
Absorption correction: multi-scan (SADABS; Krause *et al.*, 2015)	$R_{int} = 0.035$
$T_{min} = 0.522$, $T_{max} = 0.746$	$\theta_{max} = 30.6°$, $\theta_{min} = 2.3°$
14025 measured reflections	$h = -6 \rightarrow 6$
	$k = -16 \rightarrow 16$
	$l = -16 \rightarrow 19$

Refinement

Refinement on F^2	Hydrogen site location: mixed
Least-squares matrix: full	H atoms treated by a mixture of independent and constrained refinement
$R[F^2 > 2\sigma(F^2)] = 0.023$	$w = 1/[\sigma^2(F_o^2) + (0.0164P)^2 + 0.5734P]$ where $P = (F_o^2 + 2F_c^2)/3$
$wR(F^2) = 0.050$	$(\Delta/\sigma)_{max} = 0.001$
$S = 1.04$	$\Delta\rho_{max} = 0.54$ e Å^{-3}
2162 reflections	$\Delta\rho_{min} = -0.46$ e Å^{-3}
108 parameters	
2 restraints	
Primary atom site location: dual	

Special details

Geometry. All esds (except the esd in the dihedral angle between two l.s. planes) are estimated using the full covariance matrix. The cell esds are taken into account individually in the estimation of esds in distances, angles and torsion angles; correlations between esds in cell parameters are only used when they are defined by crystal symmetry. An approximate (isotropic) treatment of cell esds is used for estimating esds involving l.s. planes.

Fractional atomic coordinates and isotropic or equivalent isotropic displacement parameters (Å^2)

	x	*y*	*z*	U_{iso}*/U_{eq}
Br1	0.23474 (4)	0.47820 (2)	0.10999 (2)	0.02263 (6)
O1	0.2381 (3)	0.58496 (13)	0.49773 (10)	0.0274 (3)
O2	0.5543 (3)	0.72679 (14)	0.52156 (10)	0.0321 (3)
N1	0.1533 (3)	0.48393 (15)	0.32640 (11)	0.0198 (3)
H1A	0.109 (6)	0.481 (2)	0.3871 (7)	0.034 (7)*
H1B	0.070 (5)	0.4381 (16)	0.2809 (12)	0.027 (6)*

N2	0.4252 (3)	0.65371 (14)	0.46827 (11)	0.0196 (3)
C1	0.3467 (4)	0.56763 (15)	0.30262 (12)	0.0150 (3)
C2	0.4908 (4)	0.64946 (15)	0.36741 (12)	0.0161 (3)
C3	0.6962 (4)	0.73235 (16)	0.33831 (14)	0.0195 (4)
H3	0.7920	0.7841	0.3849	0.023*
C4	0.7603 (4)	0.73946 (16)	0.24314 (14)	0.0208 (4)
H4	0.8998	0.7958	0.2234	0.025*
C5	0.6172 (4)	0.66259 (16)	0.17556 (13)	0.0198 (4)
H5	0.6557	0.6678	0.1091	0.024*
C6	0.4222 (4)	0.57999 (15)	0.20480 (12)	0.0164 (3)

Atomic displacement parameters (Å^2)

	U^{11}	U^{22}	U^{33}	U^{12}	U^{13}	U^{23}
Br1	0.02501 (10)	0.02499 (10)	0.01769 (9)	0.00115 (8)	0.00048 (6)	−0.00340 (7)
O1	0.0283 (7)	0.0344 (8)	0.0206 (7)	−0.0053 (6)	0.0092 (5)	0.0006 (6)
O2	0.0388 (8)	0.0336 (8)	0.0241 (7)	−0.0056 (7)	0.0041 (6)	−0.0109 (6)
N1	0.0213 (7)	0.0207 (7)	0.0177 (7)	−0.0036 (6)	0.0037 (6)	0.0007 (6)
N2	0.0195 (7)	0.0209 (8)	0.0185 (7)	0.0043 (6)	0.0020 (6)	−0.0010 (6)
C1	0.0126 (7)	0.0144 (8)	0.0180 (8)	0.0035 (6)	0.0016 (6)	0.0012 (6)
C2	0.0149 (7)	0.0173 (8)	0.0162 (8)	0.0036 (6)	0.0026 (6)	0.0010 (6)
C3	0.0160 (8)	0.0161 (8)	0.0261 (9)	0.0020 (7)	0.0008 (7)	0.0003 (7)
C4	0.0169 (8)	0.0186 (9)	0.0275 (9)	0.0012 (7)	0.0050 (7)	0.0044 (7)
C5	0.0183 (8)	0.0218 (9)	0.0199 (8)	0.0051 (7)	0.0061 (6)	0.0058 (7)
C6	0.0156 (8)	0.0181 (8)	0.0154 (8)	0.0040 (6)	0.0012 (6)	−0.0009 (6)

Geometric parameters (Å, º)

Br1—C6	1.8958 (17)	C1—C6	1.426 (2)
O1—N2	1.238 (2)	C2—C3	1.399 (2)
O2—N2	1.226 (2)	C3—H3	0.9500
N1—H1A	0.878 (5)	C3—C4	1.371 (3)
N1—H1B	0.878 (5)	C4—H4	0.9500
N1—C1	1.346 (2)	C4—C5	1.399 (3)
N2—C2	1.448 (2)	C5—H5	0.9500
C1—C2	1.413 (2)	C5—C6	1.366 (2)
H1A—N1—H1B	123 (2)	C2—C3—H3	119.8
C1—N1—H1A	117.3 (16)	C4—C3—C2	120.50 (17)
C1—N1—H1B	119.4 (15)	C4—C3—H3	119.8
O1—N2—C2	119.23 (15)	C3—C4—H4	120.5
O2—N2—O1	122.05 (16)	C3—C4—C5	119.02 (17)
O2—N2—C2	118.71 (15)	C5—C4—H4	120.5
N1—C1—C2	125.66 (16)	C4—C5—H5	119.9
N1—C1—C6	120.41 (16)	C6—C5—C4	120.22 (17)
C2—C1—C6	113.93 (15)	C6—C5—H5	119.9
C1—C2—N2	121.08 (15)	C1—C6—Br1	118.06 (13)
C3—C2—N2	116.17 (16)	C5—C6—Br1	118.36 (13)

C3—C2—C1	122.73 (16)	C5—C6—C1	123.56 (16)
O1—N2—C2—C1	−0.6 (2)	C1—C2—C3—C4	1.9 (3)
O1—N2—C2—C3	177.77 (16)	C2—C1—C6—Br1	−178.24 (12)
O2—N2—C2—C1	−179.49 (16)	C2—C1—C6—C5	0.4 (2)
O2—N2—C2—C3	−1.2 (2)	C2—C3—C4—C5	0.0 (3)
N1—C1—C2—N2	−3.6 (3)	C3—C4—C5—C6	−1.6 (3)
N1—C1—C2—C3	178.20 (16)	C4—C5—C6—Br1	179.99 (13)
N1—C1—C6—Br1	1.6 (2)	C4—C5—C6—C1	1.4 (3)
N1—C1—C6—C5	−179.78 (16)	C6—C1—C2—N2	176.23 (15)
N2—C2—C3—C4	−176.44 (16)	C6—C1—C2—C3	−2.0 (2)

Hydrogen-bond geometry (Å, º)

D—H···*A*	*D*—H	H···*A*	*D*···*A*	*D*—H···*A*
N1—H1*A*···O1	0.88 (1)	1.99 (2)	2.635 (2)	130 (2)
N1—H1*A*···O1^{i}	0.88 (1)	2.43 (2)	3.201 (2)	148 (2)
N1—H1*B*···Br1	0.88 (2)	2.57 (2)	3.0432 (15)	115 (2)
C3—H3···O2	0.95	2.33	2.661 (2)	100
C5—H5···O2^{ii}	0.95	2.53	3.253 (2)	133

Symmetry codes: (i) −*x*, −*y*+1, −*z*+1; (ii) *x*+1/2, −*y*+3/2, *z*−1/2.